scientific reports

Check for updates

OPEN

Room-temperature synthesis of earth-abundant semiconductor $ZnSiN_2$ on amorphous carbon

Horácio Coelho-Júnior✉, Bruno G. Silva, Cilene Labre, Renan P. Loreto & Rubem L. Sommer

This manuscript reports room-temperature one-step synthesis of earth-abundant semiconductor $ZnSiN_2$ on amorphous carbon substrates using radio frequency reactive magnetron co-sputtering. Transmission Electron Microscopy and Rutherford Backscattering Spectrometry analysis demonstrated that the synthesis has occurred as $ZnSiN_2$ nanocrystals in the orthorhombic phase, uniformly distributed on amorphous carbon. The technique of large-area deposition on an amorphous substrate can be interesting for flexible electronics technologies. Our results open possibilities for environmentally friendly semiconductor devices, leading to the development of greener technologies.

Semiconductor materials can be considered one of the technology pillars of contemporaneous life. A great amount of work in semiconductor basic and applied science[1] has been done in the past years. In particular, nitrogen-based semiconductors revolutionized the technology of light-emitting devices[2–4]. In addition, the technological integration of those nitrides combined with semiconductor materials already used in industry is promising for manufacturing systems with multiple functionalities. Gallium nitride (GaN) synthesized by N implantation into gallium arsenide (GaAs), for example, is important for microelectronics applications[5–7].

Synthesis of eco-friendly materials is within one of the fundamental principles of green nanotechnology[8–12], which is a strong demand for a post-modern society[13], and has high socioeconomic status worldwide[14–16]. Studies on green technologies are quite recent[17] and take into consideration the long-term demand of elements[18] and its environmental impacts in the near future[19,20]. Exploring these aspects, scientists also have paid attention to abundance[21] and toxicity of elements for materials synthesis, aiming various applications[10,22–25]. Recently, studies based on computational screening followed by high-pressure synthesis, reported the discovery of a class of nitride semiconductors composed of earth-abundant elements[26]. In particular, zinc silicon nitride ($ZnSiN_2$) is a member of the ternary zinc nitride wide band gap semiconductors family[27,28]. Researchers have categorized $ZnSiN_2$ within the emerging materials class[29] as a potential candidate for photovoltaic absorber[30] and endorsed it for technological integration[31–33]. $ZnSiN_2$ synthesized by an ammonothermal approach crystallize in the orthorhombic phase and has the lattice parameters a = 5.25 Å, b = 6.28 Å and c = 5.02 Å, with a band gap of 3.7 eV at room-temperature[27]. It is important to emphasize that $ZnSiN_2$ synthesis has only a few reports in the Inorganic Crystal Structure Database to date (ICSD codes #200584[27] and #656276[28]).

In this work, we report room-temperature one-step synthesis of earth-abundant and non-toxic semiconductor $ZnSiN_2$ on amorphous carbon by using radio frequency (RF) reactive magnetron co-sputtering. The co-sputtering technique can also be suitable for dopant studies[32,34] and thus favorable to diluted magnetic semiconductors (DMS) synthesis aiming possible applications in spintronics[33,35]. Magnetron sputtering is largely applied for the deposition of a wide range of thin film materials[36,37] and it is also applicable in greener synthesis strategies[38]. Additionally, magnetic materials synthesis at room-temperature on amorphous substrates reveals a perspective for the development of flexible spintronics[39]. Our synthesis brings new perspectives to synthesize $ZnSiN_2$ without the need for expensive or complex substrate preparation or thermal treatment process. This process also has the advantage to allow large-scale/large-area synthesis, even on an amorphous substrate, a strong point to applications also in macro electronics[40,41] taking into account environmentally friendly concepts[42].

Results and discussion

In Fig. 1a, we present an ADF-STEM (Annular Dark Field-Scanning Transmission Electron Microscopy) micrograph, where is possible to observe a bright contrast corresponding to the region with the synthesized compound. This contrast comes from the nanostructures examined, which appear as bright small dots. We would like to emphasize that ADF-STEM mode was intentionally applied to maximize contrast-diffraction effects, which is possible because those nanostructures have a clear crystalline character. It is possible to observe that the bright

Brazilian Center for Physics Research, 22.290-180, Rio de Janeiro, RJ, Brazil. ✉email: hcoelhojunior@cbpf.br

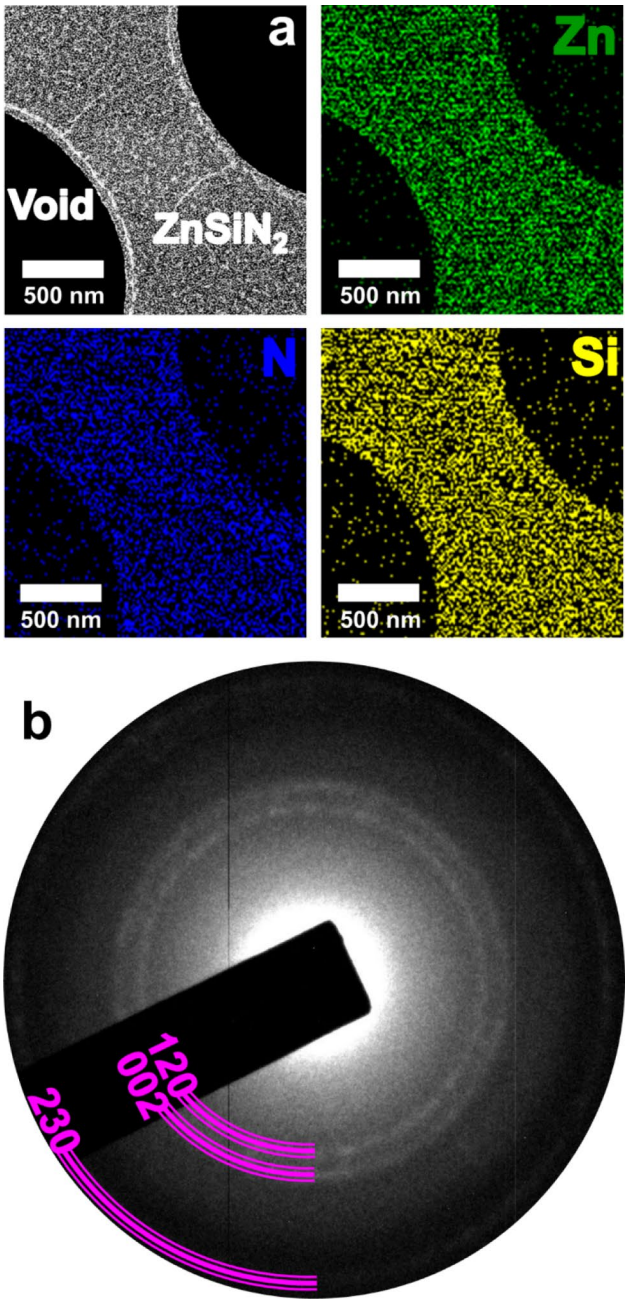

Figure 1. (**a**) ADF-STEM image and a set of EDS maps of a region with deposited $ZnSiN_2$, showing the presence of Zn (green), Si (yellow) and N (blue). (**b**) SAED pattern with the correspondent diffraction planes.

dots are evenly distributed on the amorphous carbon area. Finally, a set of EDS (Energy Dispersive X-rays Spectroscopy) maps of $ZnSiN_2$ demonstrates the uniform distribution of nanostructures on amorphous carbon, in corroboration with the ADF-STEM micrograph. Figure 1b shows a SAED (Selected Area Electron Diffraction) pattern of $ZnSiN_2$ with an annular pattern originated from nanocrystals and the amorphous substrate. Those rings are highlighted with a violet semicircle with the corresponding $ZnSiN_2$ family of planes indexed as (120), (002), and (230) of the orthorhombic phase, according to theoretical calculations for this material[27].

In Fig. 2 we detail the nanostructures presented in Fig. 1 using high magnifications. Figure 2a presents an ABF-STEM (Annular Bright Field-Scanning Transmission Electron Microscopy) micrograph showing the distribution and morphology of $ZnSiN_2$ nanostructures. The bright small dots viewed in Fig. 1a now can be seen as dark dots and demonstrate the uniform distribution of the nanostructures on amorphous carbon, reinforcing the synthesis capability by using sputtering deposition. Besides, the nanostructure sizes are practically uniform, indicating the potential for nucleation since the initial synthesis at room-temperature. This characteristic can be useful, for example, in 2D materials synthesis aiming photocatalyst applications as done in the work from Bai et al.[43]. In this study, the authors explain that $ZnSiN_2$ can have a higher band gap with respect to other zinc

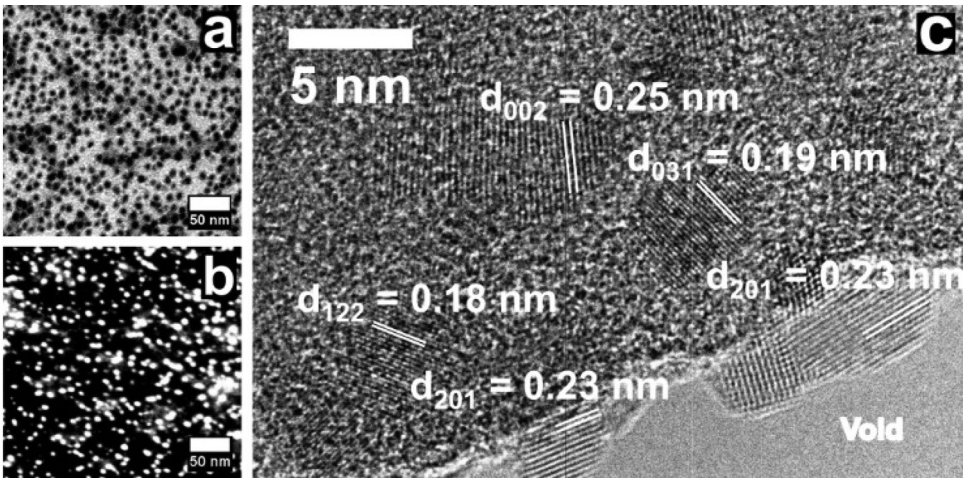

Figure 2. (**a**) ABF-STEM, (**b**) HAADF-STEM and (**c**) HRTEM micrographs of $ZnSiN_2$ nanostructures with their respective lattice spacing in its orthorhombic phase.

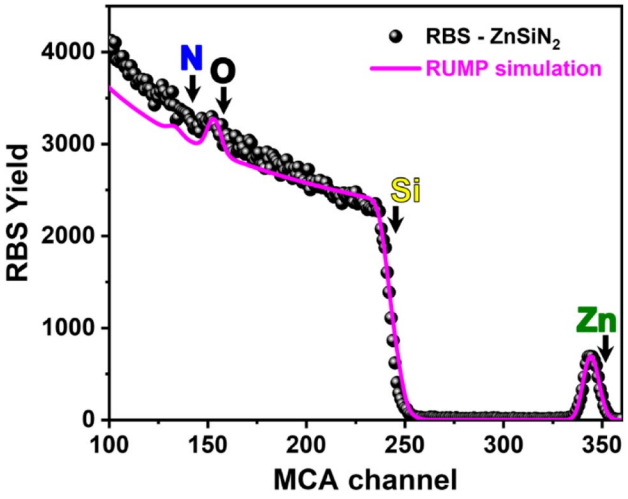

Figure 3. RBS spectrum of $ZnSiN_2$. Full circles correspond to measured RBS spectrum and line corresponds to the RBS simulation performed by RUMP code[44].

nitrides (like $ZnGeN_2$ and $ZnSnN_2$), being proposed as efficient photocatalysts for water splitting. According to the first perspective, we believe that our work opens the possibility of manufacturing devices like thin film transistor (TFT) due to the potential production of single layers with a wide band gap in a large-scale/large-area with good uniformity.

Figure 2b shows the HAADF-STEM (High-Angle Annular Dark Field) image of $ZnSiN_2$ in corroboration to Fig. 1a. Here we aim to explore variations in atomic number from elements in the sample. In this micrograph, it is possible to observe that the nanocrystals are displayed in higher contrast, because of the reduction of the contribution from amorphous carbon in the image formation. The nanocrystals observed in Fig. 1a are in agreement with HAADF measurement in Fig. 2b which show that $ZnSiN_2$ synthesis has occurred effectively. In Fig. 2c is possible to observe the interplanar spacing of $ZnSiN_2$ nanostructures distributed on amorphous carbon. This HRTEM (High-Resolution Transmission Electron Microscopy) micrograph was obtained in the region between $ZnSiN_2$/amorphous-carbon and the void, displaying the interplanar spacing that matches the crystallographic planes of the orthorhombic phase of $ZnSiN_2$[27] also in accordance with Fig. 1b.

In addition to TEM measurements, we present our quantitative analysis using RBS (Rutherford Backscattering Spectrometry). Figure 3 shows the RBS spectrum of $ZnSiN_2$ and its RBS simulation performed by the RUMP code[44]. The RBS measurement was obtained from $ZnSiN_2$ synthesized on SiO_2/Si (see Fig. 4b) complementing the qualitative EDS analysis (Fig. 1). It is possible to observe that the edge from Zn, Si, and N signals are well defined in the RBS spectrum of Fig. 3, which corroborates the presence of those elements in our synthesized material. The signals from the backscattered $^4He^{++}$ from Zn appear at around channel 344 while from Si is pronounced like a single edge around channel 242 and from N is smoothly delineated around channel 142. The RBS signal

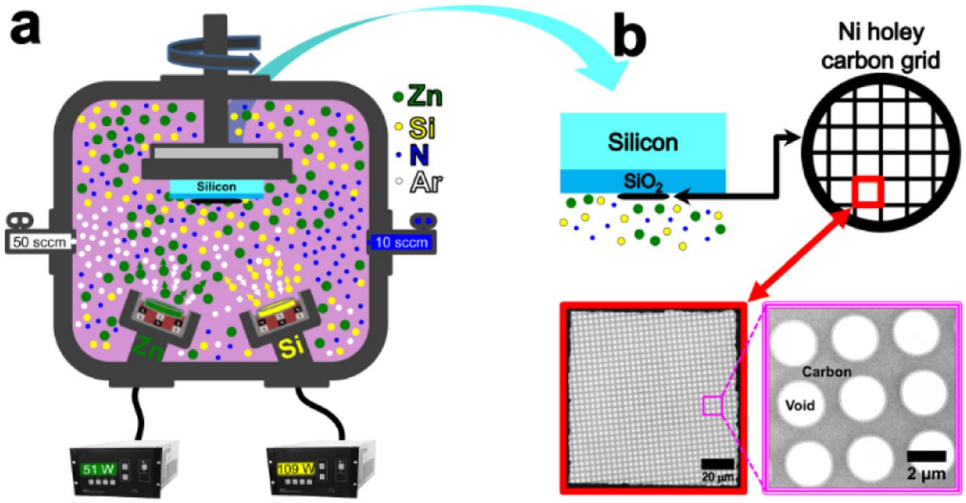

Figure 4. (**a**) Schematic setup of combinatorial sputtering for $ZnSiN_2$ synthesis on amorphous carbon. (**b**) The red square indicates a zoom from one grid quadrant while the magenta square shows a region containing amorphous carbon with circular voids.

around channel 156 is originated from oxygen in the SiO_2/Si substrate. We use a layered structure in order to effectively simulate the experimental spectrum of $ZnSiN_2$: layer 1: 7 nm of $ZnSiN_2$ layer composition; layer 2: 25 nm of SiO_2; layer 3: silicon substrate. This layered model is suitable to simulate the Zn and Si signals in the RBS spectrum, indicating the good quality of our fit. Once the sputtering technique promotes a uniform synthesis of the $ZnSiN_2$ on amorphous carbon (as demonstrated in Fig. 1), it is reasonable to expect that the synthesized $ZnSiN_2$ is also evenly distributed on SiO_2/Si. Therefore, we have demonstrated that our synthesis was successfully also in both, large-area amorphous carbon and large-area silicon oxide. It is important to point out that this work shows that we were able to promote a large-area of material synthesis through a single-step technique at room temperature, features that can be of interest for TFT technologies. In this context, is important to notice that the manufacturing of flexible TFT at room temperature using amorphous oxide semiconductors is already a reality[45]. In reference[45] the authors expressed the importance of TFT fabrication at room temperature, as well as the production in large-area for the development of flexible electronic devices. Furthermore, flexible and freestanding single layers zinc-based semiconductors, produced in large areas have been promising to enhance solar water-splitting efficiency[46], as well as for other photovoltaic applications[47,48].

Conclusion

In summary, we report room temperature one-step synthesis of earth-abundant and non-toxic semiconductor $ZnSiN_2$ on amorphous carbon substrates by using radio frequency reactive magnetron co-sputtering. The synthesis occurred as nanocrystals of $ZnSiN_2$ in its orthorhombic phase. The synthesis technique demonstrates to be capable to produce $ZnSiN_2$ in large-scale/large-area on amorphous substrates while taking into account greener concepts applied to advanced materials for flexible electronics.

Experimental section

Synthesis. $ZnSiN_2$ was synthesized by sputtering using Zn and Si targets (both with 99.99% purity) simultaneously under a mixed Ar (50 sccm) and N_2 (10 sccm) atmosphere for a nominal chamber pressure of 5 mTorr. The system base pressure was 1×10^{-7} Torr. Figure 4a shows the schematic setup of the synthesis chamber, where Zn and Si targets were kept under RF power of 51 W and 109 W, respectively. A Ni holey carbon grid (Quantifoil Q25035 R2/1 200 M) usually applied in TEM experiments was fixed on a SiO_2/silicon substrate maintained at room temperature and in constant rotation during the synthesis. Figure 4b shows the grid/substrate accommodated on the holder, highlighting the grid (~ 3 mm diameter) separately, showing the morphology of the carbon amorphous region where the $ZnSiN_2$ synthesis will be held. Before synthesis, the silicon substrate was cleaned with acetone, isopropyl alcohol, and deionized water. The carbon grid was used for TEM experiments. The material deposited on SiO_2/Si was submitted to RBS measurement.

Characterization. A JEOL FEG JEM 2100F transmission electron microscope (TEM) operated at 200-kV of acceleration voltage and equipped with an energy-dispersive x-ray spectrometer (EDS-Noran Seven) was used for HRTEM, SAED, and EDS maps. The STEM mode images were obtained using an annular dark-field (ADF) and annular bright-field (ABF) detectors. EDS measurements were performed in STEM mode. RBS was employed to evaluate the overall composition of the synthesized sample. It was carried out by using a 1.2-MeV $^4He^{++}$ ion beam produced by the 3-MV Tandetron accelerator from High Voltage Engineering Europa of the Ion Implantation Laboratory at Universidade Federal do Rio Grande do Sul (UFRGS), Brazil.

Received: 24 November 2020; Accepted: 25 January 2021
Published online: 05 February 2021

References

1. Chelikowsky, J. R. & Cohen, M. L. Semiconductors: A pillar of pure and applied physics. *J. Appl. Phys.* **117**, 112812 (American Institute of Physics Inc., 2015).
2. Service, R. F. Nitrides race beyond the light. *Science* **327**, 1598–1599 (2010).
3. Riechert, H. Lighting the 21st century. *Phys. Status Solidi* **212**, 893–896 (2015).
4. Akasaki, I. Nobel Lecture: Fascinated journeys into blue light. *Rev. Mod. Phys.* **87**, 1119 (2015).
5. Coelho-Júnior, H., dos Santos, J. H. R. & Maltez, R. L. Synthesis of a GaN nanolayer on (001) GaAs by N ion implantation. *Thin Solid Films* **642**, 129–135 (2017).
6. Coelho-Júnior, H. & Maltez, R. L. RBS/C and TEM characterization of GaN nanolayer obtained by IBS on (001) GaAs. *Nucl. Instruments Methods Phys. Res. Sect. B Beam Interact. with Mater. Atoms* **445**, 1–7 (2019).
7. Coelho-Júnior, H. & Maltez, R. L. PL characterization of GaN nanolayer obtained by N ion implantation into Si3N4/GaAs. *Opt. Mater. (Amst).* **101**, 109727 (2020).
8. Gilbertson, L. M., Zimmerman, J. B., Plata, D. L., Hutchison, J. E. & Anastas, P. T. Designing nanomaterials to maximize performance and minimize undesirable implications guided by the principles of green chemistry. *Chem. Soc. Rev.* **44**, 5758–5777 (2015).
9. Smith, G. B. Green nanotechnology: Solutions for sustainability and energy in the built environment. *J. Nanophotonics* **5**, 050201 (2011).
10. Gao, M., Shih, C. C., Pan, S. Y., Chueh, C. C. & Chen, W. C. Advances and challenges of green materials for electronics and energy storage applications: From design to end-of-life recovery. *J. Mater. Chem. A* **6**, 20546–20563 (2018).
11. Tang, S. Y., Bourne, R. A., Smith, R. L. & Poliakoff, M. The 24 principles of green engineering and green chemistry: "IMPROVEMENTS PRODUCTIVELY". *Green Chem.* **10**, 268–326 (2008).
12. Anastas, P. T. & Zimmerman, J. B. The periodic table of the elements of green and sustainable chemistry. *Green Chem.* **21**, 6545–6566 (2019).
13. Graedel, T. E., Harper, E. M., Nassar, N. T. & Reck, B. K. On the materials basis of modern society. *Proc. Natl. Acad. Sci. U. S. A.* **112**, 6295–6300 (2015).
14. Kolotzek, C., Helbig, C., Thorenz, A., Reller, A. & Tuma, A. A company-oriented model for the assessment of raw material supply risks, environmental impact and social implications. *J. Clean. Prod.* **176**, 566–580 (2018).
15. Hallstedt, S. I. & Isaksson, O. Material criticality assessment in early phases of sustainable product development. *J. Clean. Prod.* **161**, 40–52 (2017).
16. Vesborg, P. C. K. & Jaramillo, T. F. Addressing the terawatt challenge: Scalability in the supply of chemical elements for renewable energy. *RSC Advances* **2**, 7933–7947 (2012).
17. Barbieri, N., Marzucchi, A. & Rizzo, U. Knowledge sources and impacts on subsequent inventions: Do green technologies differ from non-green ones?. *Res. Policy* **49**, 103901 (2020).
18. Watari, T., Nansai, K. & Nakajima, K. Review of critical metal dynamics to 2050 for 48 elements. *Resour. Conserv. Recycl.* **155**, 104669 (2020).
19. Zimmerman, J. B., Anastas, P. T., Erythropel, H. C. & Leitner, W. Designing for a green chemistry future. *Science* **367**, 397–400 (2020).
20. Johnson, A. C., Jin, X., Nakada, N. & Sumpter, J. P. Learning from the past and considering the future of chemicals in the environment. *Science* **367**, 384–387 (2020).
21. Matlin, S. A., Mehta, G., Hopf, H. & Krief, A. The periodic table of the chemical elements and sustainable development. *Eur. J. Inorg. Chem.* **2019**, 4170–4173 (2019).
22. Rosales, B. A., White, M. A. & Vela, J. Solution-grown sodium bismuth dichalcogenides: Toward earth-abundant biocompatible semiconductors. *J. Am. Chem. Soc.* **140**, 3736–3742 (2018).
23. Kuhar, K., Pandey, M., Thygesen, K. S. & Jacobsen, K. W. High-throughput computational assessment of previously synthesized semiconductors for photovoltaic and photoelectrochemical devices. *ACS Energy Lett.* **3**, 436–446 (2018).
24. Reiss, P., Carrière, M., Lincheneau, C., Vaure, L. & Tamang, S. Synthesis of semiconductor nanocrystals, focusing on nontoxic and earth-abundant materials. *Chem. Rev.* **116**, 10731–10819 (2016).
25. Alharbi, F. *et al.* Abundant non-toxic materials for thin film solar cells: Alternative to conventional materials. *Renew. Energy* **36**, 2753–2758 (2011).
26. Hinuma, Y. *et al.* Discovery of earth-abundant nitride semiconductors by computational screening and high-pressure synthesis. *Nat. Commun.* **7**, 11962 (2016).
27. Häusler, J., Schimmel, S., Wellmann, P. & Schnick, W. Ammonothermal synthesis of earth-abundant nitride semiconductors ZnSiN2 and ZnGeN2 and dissolution monitoring by in situ X-ray imaging. *Chem. A Eur. J.* **23**, 12275–12282 (2017).
28. Endo, T., Sato, Y., Takizawa, H. & Shimada, M. High-pressure synthesis of new compounds, ZnSiN2 and ZnGeN2 with distorted wurtzite structure. *J. Mater. Sci. Lett.* **11**, 424–426 (1992).
29. Oba, F. & Kumagai, Y. Design and exploration of semiconductors from first principles: A review of recent advances. *Appl. Phys. Express* **11**, 060101 (2018).
30. Pandey, M., Kuhar, K. & Jacobsen, K. W. II-IV-V2 and III-III-V2 polytypes as light absorbers for single junction and tandem photovoltaic devices. *J. Phys. Chem. C* **121**, 17780–17786 (2017).
31. Lyu, S. & Lambrecht, W. R. L. Band alignment of III-N, ZnO and II-IV-N2 semiconductors from the electron affinity rule. *J. Phys. D. Appl. Phys.* **53**, 015111 (2020).
32. Adamski, N. L., Wickramaratne, D., Wickramaratne, D. & Van De Walle, C. G. Band alignments and polarization properties of the Zn-IV-nitrides. *J. Mater. Chem. C* **8**, 7890–7898 (2020).
33. Erwin, S. C. & Žutić, I. Tailoring ferromagnetic chalcopyrites. *Nat. Mater.* **3**, 410–414 (2004).
34. Walsh, A. & Zunger, A. Instilling defect tolerance in new compounds. *Nat. Mater.* **16**, 964–967 (2017).
35. Rufinus, J. Magnetic properties of M-doped (M=Mn, Cr, or V) ZnSiN2. *J. Appl. Phys.* **105**, 07C509 (2009).
36. Kelly, P. & Arnell, R. Magnetron sputtering: A review of recent developments and applications. *Vacuum* **56**, 159–172 (2000).
37. Mavukkandy, M. O. *et al.* Thin film deposition techniques for polymeric membranes: A review. *J. Memb. Sci.* **610**, 118258 (2020).
38. Gang, M. G. *et al.* Sputtering processed highly efficient Cu_2 ZnSn(S, Se)4 solar cells by a low-cost, simple, environmentally friendly, and up-scalable strategy. *Green Chem.* **18**, 700–711 (2016).
39. Ansari, M. S., Othman, M. H. D., Ansari, M. O., Ansari, S. & Abdullah, H. Reactively sputtered half-metallic Fe3O4 thin films at room temperature on polymethyl methacrylate: A perspective for flexible spintronics. *Ceram. Int.* **46**, 19302–19310 (2020).
40. Reuss, R. H. *et al.* Macroelectronics: Perspectives on technology and applications. *Proc. IEEE* **93**, 1239–1256 (2005).
41. Ahn, J.-H. *et al.* Heterogeneous three-dimensional electronics by use of printed semiconductor nanomaterials. *Science* **314**, 1754–1757 (2006).
42. Wang, P. *et al.* The evolution of flexible electronics: from nature, beyond nature, and to nature. *Adv. Sci.* **7**, 2001116 (2020).
43. Bai, Y. *et al.* Single-layer $ZnMN_2$ (M = Si, Ge, Sn) Zinc nitrides as promising photocatalysts. *Phys. Chem. Chem. Phys.* **20**, 14619–14626 (2018).

44. Doolittle, L. R. A semiautomatic algorithm for rutherford backscattering analysis. *Nucl. Instruments Methods Phys. Res. Sect. B Beam Interact. with Mater. Atoms* **15**, 227–231 (1986).
45. Nomura, K. *et al.* Room-temperature fabrication of transparent flexible thin-film transistors using amorphous oxide semiconductors. *Nature* **432**, 488–492 (2004).
46. Sun, Y. *et al.* Fabrication of flexible and freestanding Zinc chalcogenide single layers. *Nat. Commun.* **3**, 1057 (2012).
47. Li, J. *et al.* Ternary CuZnS nanocrystals: Synthesis, characterization, and interfacial application in perovskite solar cells. *Inorg. Chem.* **57**, 8375–8381 (2018).
48. Duan, C. *et al.* Facile preparation and characterization of ZnCdS nanocrystals for interfacial applications in photovoltaic devices. *J. Colloid Interface Sci.* **512**, 353–360 (2018).

Acknowledgements

H. C.-Júnior and R. L. Sommer acknowledge financial support from Brazilian agencies: Fundação de Amparo à Pesquisa do Estado do Rio de Janeiro (FAPERJ), Conselho Nacional de Desenvolvimento Científico e Tecnológico (CNPq) and Financiadora de Estudos e Projetos (FINEP). The authors would like to thank Laboratório Multiusuário de Nanociência e Nanotecnologia (LABNANO) and Laboratório de Superfícies e Nanoestruturas from CBPF. The authors also are grateful by RBS experiment performed using the facilities of the Ion Implantation Laboratory at UFRGS. In addition, H. C.-Júnior would like to express their sincere thanks to Professors H. I. Boudinov of the Institute of Physics at UFRGS and A. L. Rossi of the CBPF for their helpful discussions.

Author contributions

H.C.-J. conceived the idea of this work and wrote the manuscript. H.C.-J., R.P.L., and B.G.S performed the sputtering synthesis. H.C.-J. and C.L. performed the TEM characterization. H.C.-J. performed the RBS analysis. R. L. S. organized and supervised the work. All authors discussed the results and revised the manuscript to the final format.

Competing interests

The authors declare no competing interests.

Additional information

Correspondence and requests for materials should be addressed to H.C.-J.

Reprints and permissions information is available at www.nature.com/reprints.

Publisher's note Springer Nature remains neutral with regard to jurisdictional claims in published maps and institutional affiliations.